BULETINUL INSTITUTULUI POLITEHNIC DIN IAŞI
Publicat de
Universitatea Tehnică „Gheorghe Asachi” din Iaşi
Volumul 68 (72), Numărul 1, 2022
Secţia
CONSTRUCŢII. ARHITECTURĂ
DOI: 10.2478/bipca-2022-0007

# CYCLIC TESTING OF BEAM TO COLUMN DOWEL CONNECTION

BY

**MARIUS GEORGE LUCIAN MOLDOVAN* and MIHAI NEDELCU**

Technical University of Cluj-Napoca, Faculty of Civil Engineering, *15 C Daicoviciu Str., 400020, Cluj-Napoca, Romania*

Received: March 29, 2023
Accepted for publication: July 18, 2023

**Abstract.** This study investigates the behaviour and failure mechanisms of beam-to-column dowel connections in precast industrial halls under lateral loads. Two large-scale cyclic tests were performed to evaluate the assembly failure and its relationship with the dowel connection. The results demonstrated that the assembly failure coincided with the dowel connection failure, governed by dowel yielding and concrete spalling of the column fork. No significant damage was observed in the concrete elements outside the connection area. The dissipative failure mechanism of the column was not achieved, indicating that this dowel connection is not capable to transmit sufficient lateral load. The maximum capacity of the dowel connection was influenced by the concrete coverage of the dowel in relation to the side of the column fork. This research serves as a basis for further investigation and potential improvements in the design and performance of connections in precast concrete structures.

**Keywords:** Structural behaviour, lateral loads, failure mechanisms, precast concrete, large-scale experiments.

*Corresponding author; *e-mail*: george.moldovan@mecon.utcluj.ro
© 2022 Marius George Lucian Moldovan and Mihai Nedelcu
This is an open access article licensed under the Creative Commons Attribution-NonCommercial-NoDerivatives 4.0 International license (CC BY-NC-ND 4.0).

## 1. Introduction

In the aftermath of World War II, the reconstruction period saw a surge in popularity for precast industrial buildings.. This preference arose from the pressing need to efficiently and economically expand infrastructure while contending with the scarcity of materials and workforce during that time. Consequently, precast techniques were solidified and continued to be employed without substantial changes to connection methods across numerous European countries. This led to a widespread presence of industrial structures (Fig. 1) characterized by slender cantilever columns connected through high-span beams .

Beam-to-column dowel connections are widely used, in Europe, in precast single-story concrete structures to transfer lateral loads between different structural components. Such connections are composed of dowel bars that transmit shear forces and bending moments. The ability of these connections to resist lateral loads is crucial for the overall performance of the structure, as they must withstand cyclic actions from natural hazards like wind and earthquakes without collapsing. Nonetheless, these connections are prone to failure due to several factors, including inadequate design, deficient code prescriptions, or poor understanding of the failure mechanism.



Fig. 1 – Common precast industrial buildings structure.

Typically, beam-to-column dowel connections are designed with only execution, gravity and wind loads in mind . However, in seismic zones, current design principles are insufficient, and additional factors must be considered when designing these connections. For instance, the support length of the beam and the dimensions of the dowels used to secure the connections are essential parameters that may impact the overall structure's behaviour.

The capacity of dowel connections can be assessed through experimental testing or numerical modelling. Full-scale testing is more realistic but more expensive and time-consuming, while small-scale testing is more practical but may not fully replicate the behaviour of dowel connections under real-world loading conditions. Numerical models can simulate the dowel connection's performance under different loading scenarios, including dowel size and spacing, concrete strength, and other factors, but they must be validated by experimental results.

In Europe, the COST C1 action , which included participation from over 125 research centers across 25 countries, investigated the performance of semi-rigid connections, with a minor focus on precast connections. Additionally, the Tampere University of Technology in Finland carried out full-scale experiments on portal frames to assess the response of beam-to-column connections under lateral loads . Although the topic regarding the behaviour of the connections in precast structures was proposed, there was still a lack of sufficient experimental tests demonstrating the overall performance of precast structures which resulted in the exclusion of precast systems from the first edition of Eurocode 8 . To address these limitations, new projects were initiated among European associations, as summarized by G. Toniolo . The Ecoleader project examined two full-scale structural prototypes, comparing a precast system with hinged beam-to-column connections to similar cast in situ structures. This project represented a significant milestone for the European precast industry, as its findings contributed to the inclusion of precast frame systems in Eurocode 8 .

The SAFECAST project on “Design Guidelines for Connections of Precast Structures under Seismic Actions” which explored the vulnerability of precast connections during earthquakes, states that any connection type must undergo initial type testing to quantify its strength and potentially other properties affecting its seismic behaviour, this implies that extensive study of a precast connection's behaviour through experimental and numerical testing is required before its. As part of this project, Bournas et al. examined the performance of a full-scale three-story structure subjected to seismic loading, focusing specifically on the behaviour of mechanical beam-to-column connectors. They tested and compared a commonly used pinned beam-to-column connection in European countries (involving steel dowel bars) with an innovative dry mechanical connection designed to emulate beam-to-column connections. Their findings revealed that the newly proposed solution demonstrated superior capacity, underscoring the importance of continued research and development of novel solutions for precast structural connections. To suggest and develop new solutions, it is essential to comprehend the failure mechanisms of the current connections. In the case of dowel connections, which are prevalent in Europe, failure sources are associated with friction strength for structures designed to handle vertical loads. Furthermore, inadequate detailing of connectors and their

surrounding areas is the result of a limited understanding of their behaviour and a lack of code requirements and prescriptions .

Zoubek et al. have noted that most previous studies have primarily concentrated on the local failure of dowels, complicating the application of certain design recommendations for structures in seismic zones where global failure could occur. Nonetheless, some researchers have utilized resources such as the Precast Seismic Structural Systems (PRESSS) project to examine precast structures by conducting large-scale tests to evaluate the seismic behaviour of precast buildings. The main objective of this research was to establish design guidelines to increase the acceptance of precast concrete structures in seismic regions and to devise new materials, ideas, and techniques for areas with high seismic activity. Another European project, "Precast EC8: Seismic behaviour of precast concrete structures with respect to Eurocode 8 (Co-Normative Research)" which was completed in 2007 , focused on the overall behaviour and ductility of precast structures, without examining the seismic behaviour of specific connections, leaving many questions unanswered.

Numerous existing precast structures in Southern Europe's seismic regions were constructed without appropriate seismic detailing for connections, often depending on dry friction resistance joints . At the time, non-seismic codes permitted dry-friction connections, which resulted in significant relative displacements and increased collapse risk Updated codes in seismically active countries now prohibit the use of friction-based connections. Experimental tests have demonstrated that the neoprene-concrete friction coefficient ranges from 0.09 to 0.13 , which is often insufficient to withstand shear forces from horizontal wind actions . In many instances involving simple pinned connections relying on friction, connection failure will occur before the formation of dissipative plastic hinges at the column bases . Observations from recent seismic events, particularly in the Emilia Romagna region of Italy , highlight that precast connections still represent a significant vulnerability during earthquake. These observations gained additional support from the analysis of the 1999 Kocaeli earthquake in Turkey which revealed that over 50% of local industrial buildings experienced structural damage Precast structures, which made up 90% of these facilities, were particularly vulnerable due to insufficient stiffness and ductility in their connections . In the same earthquake, incomplete precast structures experienced complete collapse, demonstrating inadequate connections between their components. Similar findings emerged from the more recent L'Aquila earthquake in Italy, where precast structures' beams and columns were damaged, with the most critical areas being the connections between elements, resulting in beam unseating . It was determined that precast structures are more susceptible to damage during seismic events compared to cast-in-place reinforced concrete structures . Due to these seismic events there is an increased focus on reducing seismic risk and understanding the performance of commonly implemented solutions. In this sense the fib Bulletins 27 and 48 (Task Group 6.12: fib Design

Handbook) offer equations for estimating dowel connection capacities which can be considered at a local level and under the condition that all other requirements, such as adequate concrete coverage, are met. Some researchers have further explored the behaviour of dowel connections with the primary goal of devising methods to assess the capacity of these joints , but due to the lack of standardization for precast structures, small changes in the geometry of the connection can significantly alter their capacity. Consequently, despite the numerous studies on precast connections, available data remains limited, and additional monotonic and cyclic research is needed, particularly for commonly used connection types There is currently no consensus on ductility, stiffness, and hysteretic behaviour. Many factors, such as concrete coverage and force direction acting on the connection during seismic actions, are not considered in existing connection designs. Experimental tests have revealed that dowel connection capacity is reduced by 50% during cyclic tests compared to monotonic tests .

The need for further experimental research to verify the common connection solutions in practice is evident . Various researchers have conducted cyclic and dynamic tests on different connection sub-assemblies , and when combined with full-scale prototype tests at the ELSA laboratory, it has been demonstrated that conventional dynamic modal analysis with response spectrum may underestimate the internal forces in the structures and their connections. This conclusion is further supported by advanced nonlinear finite element models calibrated using experimental results . A similar study was conducted in order to evaluate the strength of dowel connections , adhering to the SAFECAST guidelines . Despite numerous tests, the conclusion was that it remains challenging to draw universally applicable capacity estimations for all connection types. This is primarily due to the existence of untested parameters in realistic connections, indicating the need for additional research.

## 2. Experimental procedure description

The literature review reveals numerous beam-to-column connection configurations, with minor geometric changes potentially affecting the connection's lateral load capacity. This makes it challenging to accurately assess the capacity of the connections based solely on design code information. Consequently, this research focused on experimentally investigating a dowel connection commonly used in Romania's precast industry. As illustrated in Fig. 2, the dowel is embedded in the precast column forks and inserted into sleeves within the beam flanges. These sleeves are grouted to establish a mechanical connection and ensure proper force transmission under lateral loads. The study

aims to examine the failure mechanism of the proposed assembly through cyclic loading.



Fig. 2 – Precast structure using beam-to column dowel connection.

Due to the significant size of precast elements, some adaptations were necessary for laboratory testing and handling. The objective was to minimize these modifications to accurately capture the behaviour of a real-life precast frame structure with beam-to-column dowel connection. However, the adaptations should not impact the assembly's overall. For this experimental investigation, an end column supporting a single main beam was selected. The specimens' general dimensions are displayed in Fig. 3.

The column length was reduced from 8.5m to 6m, and to achieve equivalent top displacements and rotations, the cross-section was also reduced from 80x80cm to 60x60cm. The chosen beam length of approximately 3m was determined by the same laboratory constraints and to prevent local effects on the connection from load application at the beam's opposite end. Prestressed concrete beams can exceed 20m in length.

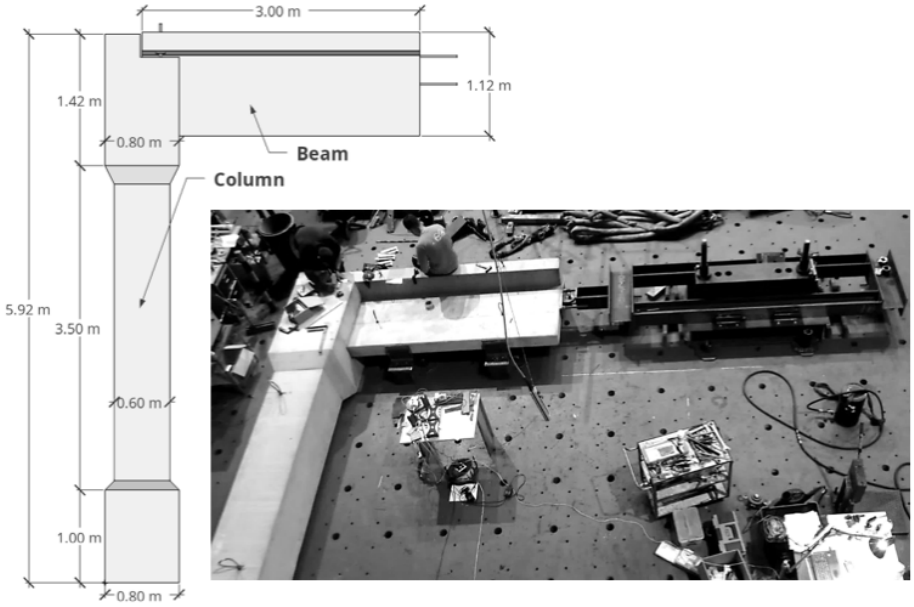



Fig. 3 – General dimension of the test specimens.

Owing to the considerable dimensions of the specimens and the need to prioritize safety, the tests were carried out horizontally on the laboratory floor. This approach, however, introduces a downside as it creates extra friction on the sides of both the column and the beam that come into contact with the floor. This added friction could potentially affect the test results, as it might not accurately represent the actual conditions that would be encountered in a real-life vertical setup. Despite this drawback, the horizontal testing method remains necessary to ensure the safe handling and testing of large specimens within the laboratory. The testing setup is shown in Fig. 4. Greased steel plate sets were placed beneath all moving components to minimize friction as effectively as possible. The column was secured at its base with steel structures that mimic actual pocket foundations. A separate steel structure was utilized to apply force at the beam's end, allowing for the hydraulic jack's installation across the "reaction wall" to conduct the cyclic analysis.

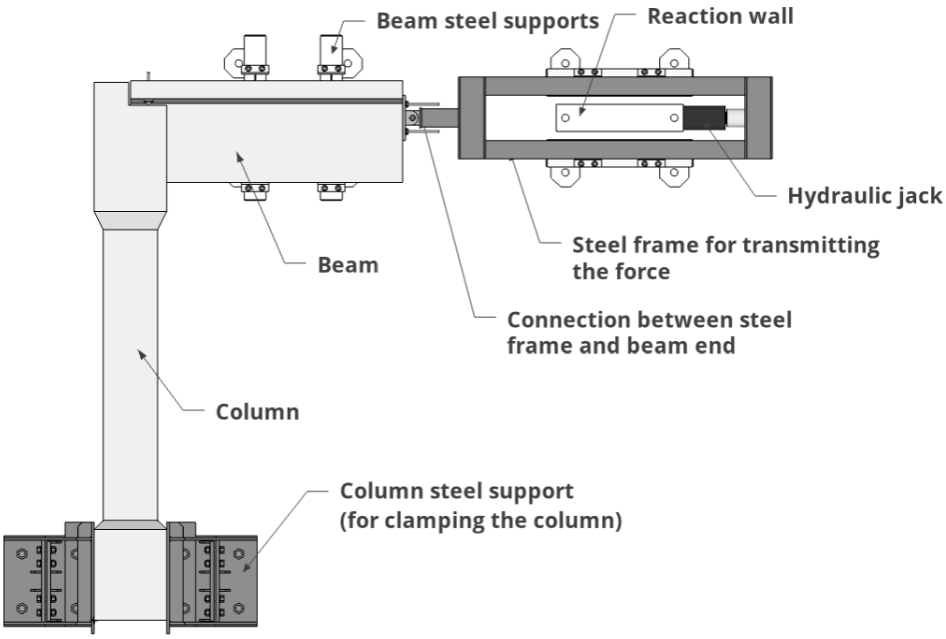



Fig. 4 – Top view of the testing setup.

Two sets of cyclic loading tests were performed during this research. To obtain a wider range of results and to evaluate the dowel concrete coverage effect on the capacity of the connection the size of the column fork and the web of the beam web were different between the two sets of tests. The dimensions of the column fork and the beam end, as well as the positions of the dowels and connection holes in the beam for the first set (CT1) can be seen in Fig. 5 and Fig. 6. The column forks were 29cm thick and the beam web 18cm thick. In this common connection setup, the dowels are placed fairly near the inner side of the fork, with just 7cm of concrete cover between the dowel's centerline and the inner edge, and 20cm to the front edge. For the second set of test (CT2) the column forks were 23cm thick and the beam web 30cm thick, the dimensions of these specimens can be seen in Fig. 7 and Fig. 8. For both tests dowels of 32mm diameter were used.

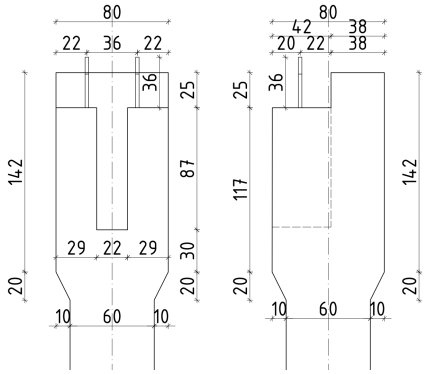



Fig. 5 CT1 – Column fork dimensions and dowels position.

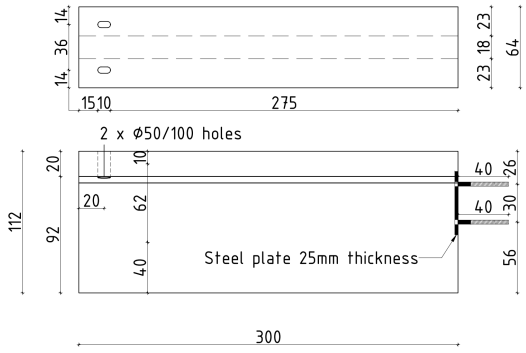



Fig. 6 CT1 – Beam dimensions and hole position.

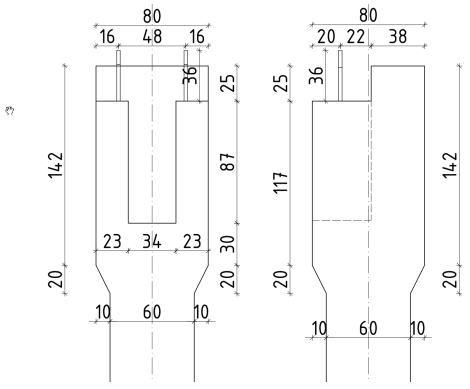



Fig. 7 CT2 – Column fork dimensions and dowels position.

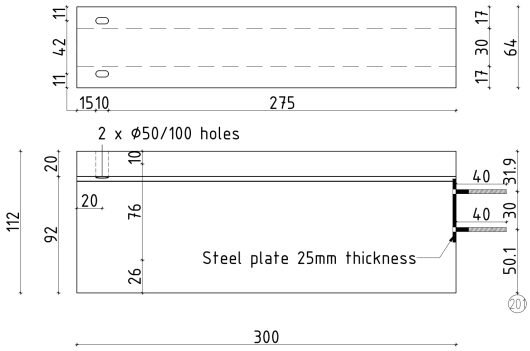



Fig. 8 CT2 – Beam dimensions and hole position.

Loading was performed based on the description offered in the SAFECAST testing protocol. The load was applied along the beam's axis. Depending on whether the test was monotonic or cyclic, the load was either unidirectional (tensile force) or bidirectional (tension and compression). To alter the direction of the load, the hydraulic jack was repositioned to the opposite side of the reaction wall, pushing the steel frame and transferring the force to the beam in the opposite direction. The maximum displacement (at failure) was obtained from an initial monotonic test. Based on these results where failure occurred at a maximum top displacement of 180mm for the cyclic tests the load displacement was divided into three increment groups, 60mm, 120mm and 180mm. The loading protocol is shown in Fig. 9.

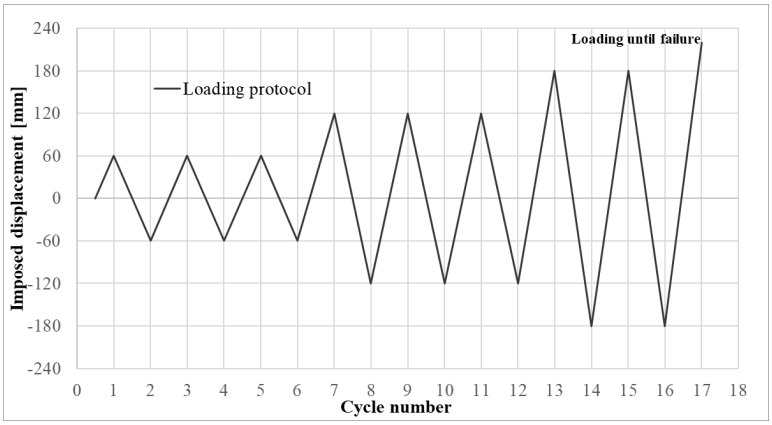



Fig. 9 – Cyclic loading protocol.

Two QUANTUM MX840B measurement amplifiers were employed for data collection. A total of 16 channels were measured, with data recorded at a

10Hz sampling rate. The positions of the measuring equipment for the CT1 experiment can be seen in Fig. 10, which also indicates the locations of the strain gauges (SG) and the force/displacement transducers (CH). CH1 and CH2 transducers measure the relative displacement between the column fork and the beam end. For the test CT2, the locations of certain strain gauges were adjusted based on the outcomes of the prior test, CT1. As some strain gauges did not record significant data, they were relocated to areas where most damage had been observed in previous tests, the positions of the measuring equipment for the second test can be seen in Fig. 11.

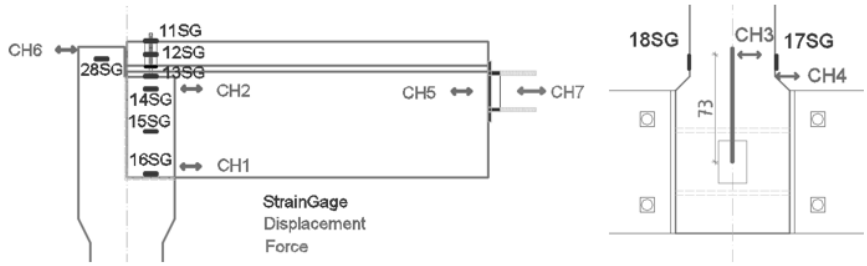



Fig. 10 CT1 – Measuring equipment position.

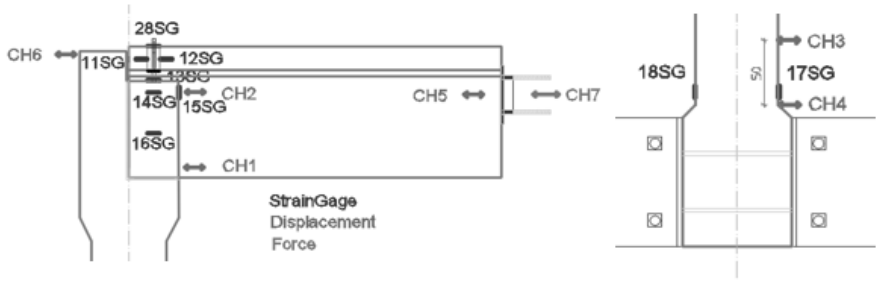



Fig. 11 CT2 – Measuring equipment position.

While casting the test elements, concrete samples were gathered. The material properties of these samples were determined according to Eurocode guidelines on the testing day, included compressive strength (for both cubes and cylinders), tensile strength, and modulus of elasticity (refer to Table 1 and Table 2). As you can observe from Table 1 and Table 2, high strength concrete was used for both column and beam. Usually in normal practice, prestressed beams use such a high class of concrete (C50/60) and the columns are usually casted using a C35/45 concrete class. The material properties were determined from three separate sets of tests for each testing assembly. The reinforcements, such as the dowels, utilized S500B steel class with average properties of $f_y$=561MPa,

$f_u$=656MPa, and $\varepsilon_u$=10.73%. The dowels were grouted with the Sika AnchorFix®-3030 product .

**Table 1**

*Concrete compressive strength*

| Specimen | | Compressive strength cube ($f_c$) | Average cube ($f_{cm}$) | Compressive strength cylinder ($f_c$) | Average cylinder ($f_{cm}$) |
|---|---|---|---|---|---|
| | | (MPa) | (MPa) | (MPa) | (MPa) |
| CT1 | 1 | 74.26 | 71.25 | 59.5 | 60.9 |
| | 2 | 66.27 | | 57.8 | |
| | 3 | 73.23 | | 65.2 | |
| CT2 | 1 | 76.07 | 75.70 | 67.5 | 65.4 |
| | 2 | 73.96 | | 64.4 | |
| | 3 | 77.07 | | 64.3 | |

**Table 2**

*Concrete tensile strength and elasticity modulus*

| Specimen | | Tensile strength ($f_{cf}$) | Average ($f_{cf.m}$) | Elasticity modulus ($E_c$) | Average ($E_{cm}$) |
|---|---|---|---|---|---|
| | | (MPa) | (MPa) | (MPa) | (MPa) |
| CT1 | 1 | 4.69 | 4.8 | 26218 | 28367 |
| | 2 | 4.9 | | 30232 | |
| | 3 | - | | 28652 | |
| CT2 | 1 | 4.97 | 4.94 | 37281 | 39079 |
| | 2 | 4.73 | | 44597 | |
| | 3 | 5.11 | | 35361 | |

## 3. Test results for the first cyclic test (CT1)

For the first cyclic test, CT1, there was no visible damage in the first 12 cycles (Fig. 9). Notable cracks emerged around the joint during the 13th loading cycle, Fig. 12 shows the initial crack appearing on the column fork corresponding to a load of about 249kN. This crack expanded during subsequent cycles and was accompanied by smaller cracks in the same area. On the beam side, there were numerous small cracks, but none were as large as those on the column fork. Dowel deformation became more apparent after the first cracks emerged, suggesting internal debonding of the components. During the 17th cycle, the specimens were loaded until failure, which occurred suddenly due to a combination of steel dowel yielding and concrete spalling around the dowel in

the column fork (Fig. 13). The maximum recorded load at failure was roughly 270kN.

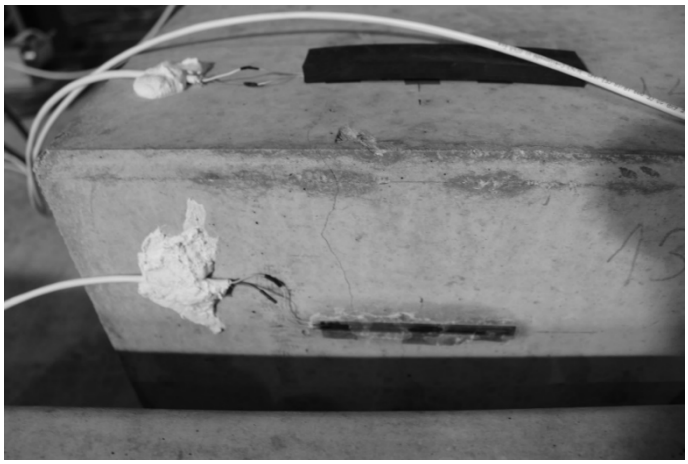


Fig. 12 CT1 – First crack in the area of the connection.

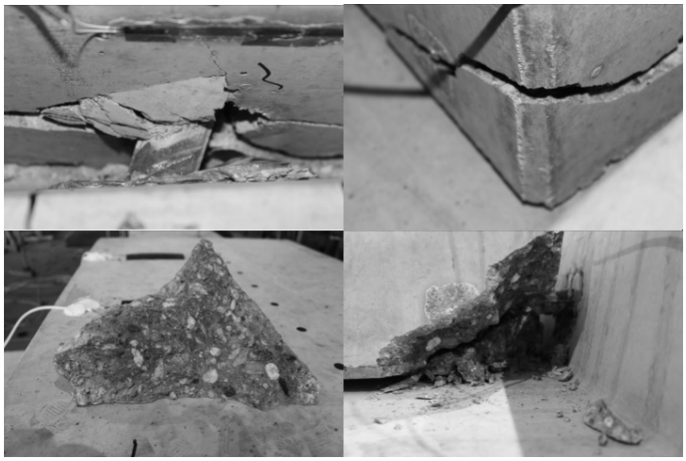


Fig. 13 CT1 – Failure mechanism.

During the last loading cycle, the damage around the dowel grew exponentially, progressing from minor concrete crushing to sudden concrete spalling, which is clearly visible by comparing Fig. 12 with Fig. 13. The damage around the dowel in the beam hole area was limited and less significant due to the high strength of the material used for injection. The initial conclusion suggests that the 70mm lateral concrete coverage of the dowel is inadequate for this specific connection, as no other significant damage was observed elsewhere in

the assembly. Connection failure should typically occur after the formation of a plastic hinge at the column base, which is the intended dissipation mechanism for such structures. Outside the connection area, the maximum crack width was located at the column base which was approximately 0.60mm at failure. This suggests that the column itself did not suffer significant damage, and the assembly failure was directly related to the connection failure.

The observed failure was comparable on both sides of the column. The test was halted for safety reasons and to avoid damage to the testing equipment once the concrete had spalled. Just before stopping completely, the displacement increased while the loading force decreased. Although the dowel connection did not experience a full rupture, it was significantly damaged and could not handle superior loads. In a real-world scenario, this could be a precursor to a progressive collapse if the displacement continues to grow and the beam becomes unseated from the column. The plastic hinge's location was roughly 8cm inside the column fork for both dowels (Fig. 14), and a longer free length of the dowel, due to the unbonding inside the concrete elements, reduced the connection's maximum capacity. The capacity of the dowel is influenced by the length between the two elements. When the distance between the two concrete elements is close to zero, forces are mainly transmitted through shear forces; however, as the value increases, the effect of the catenary action becomes significant, inducing longitudinal tension forces inside the dowels and reducing the maximum capacity of the connection.

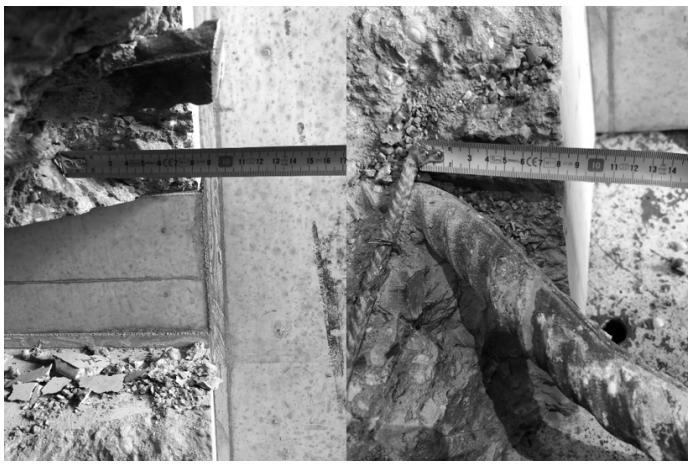


Fig. 14 CT1 – Position of the dowel plastic hinge inside the column fork.

Measurements from CH1 and CH2 (Fig. 15 and Fig. 16) reveal that under lateral compression, the relative displacement between the column fork and the beam is considerably smaller than under tension. This can be attributed to the concrete-to-concrete contact between the two sizable components. CH1

registered a larger displacement in both compression and tension, as this transducer was situated near the column fork's bottom, while dowel connectors were positioned at the top of the fork, effectively diminishing the maximum displacement in that region, as demonstrated by CH2 measurement. The elevated relative displacements in tension at the fork's bottom further support the hypothesis that, under higher loads, the beam could potentially become unseated and expedite the assembly's damage.

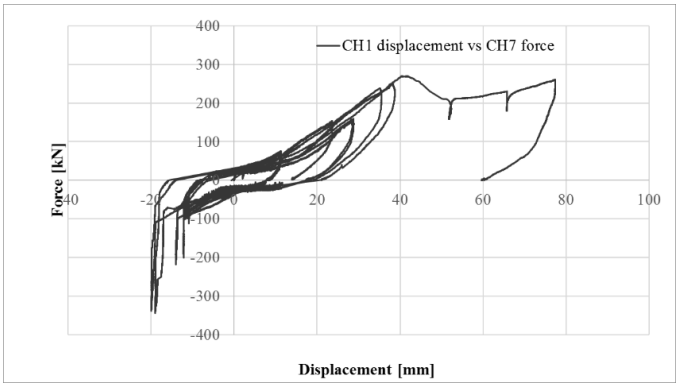



Fig. 15 CT1 – Transducer CH1 measurement.

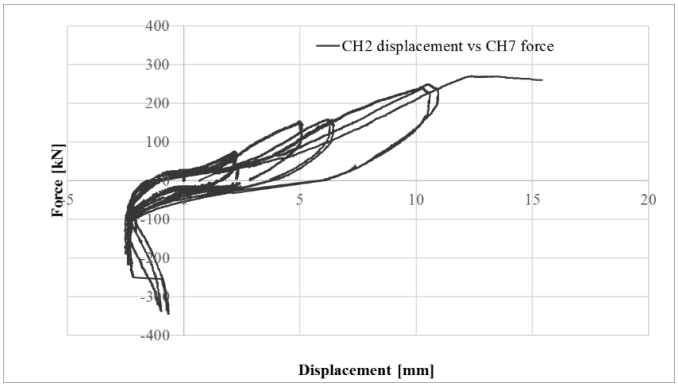



Fig. 16 CT1 – Transducer CH1 measurement.

The transducers located at the base of the column, CH3 and CH4, reveal the free rotation of the assembly due to the imperfect floor attachment; the measurements are shown in Fig. 17 and Fig. 18. This rotation persisted and it was more pronounced during earlier cycles until the fixing assembly settled into position. The failure mechanism of the assembly remained unaffected, as the column's fixing assembly still provided adequate strength to secure the base in place. The imperfect base attachment resulted in higher-than-anticipated top

displacements, which were recorded by CH5 and CH6 transducers. The data indicates an initial lower stiffness corresponding to the first cycles, up to approximately 60mm displacement, during which the assembly consolidates under loading. This is followed by a near-linear increase in stiffness for subsequent cycles until the abrupt failure.

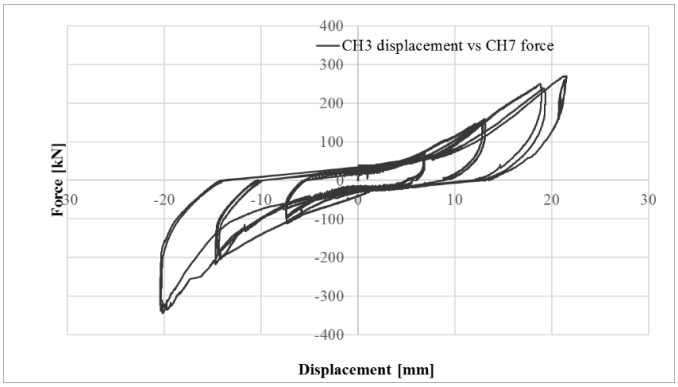



Fig. 17 CT1 – Transducer CH3 measurement.

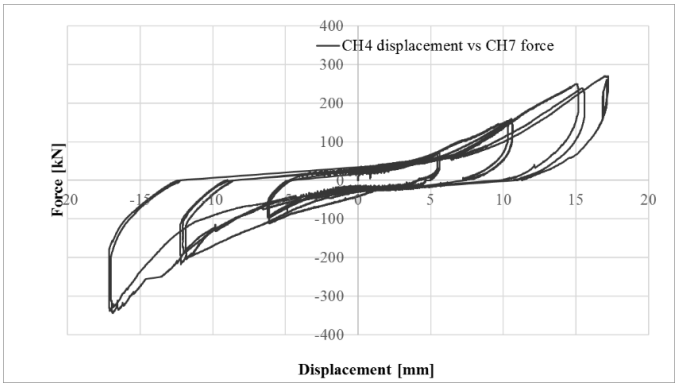



Fig. 18 CT1 – Transducer CH4 measurement.

During the final loading cycle leading to failure, the results exhibit a sudden strength reduction at around 200mm displacement (Fig. 19). Although loading was attempted to continue, another abrupt drop followed, signifying a low remaining capacity, and the test was terminated for safety reasons. The initial snapback behaviour exhibited by both CH5 and CH6 results (Fig. 19 and Fig. 20) coincided with the initial concrete spalling around the dowel connection. During the second loading attempt, the insufficient coverage led to further concrete damage and a continuous increase in the dowels' free length.

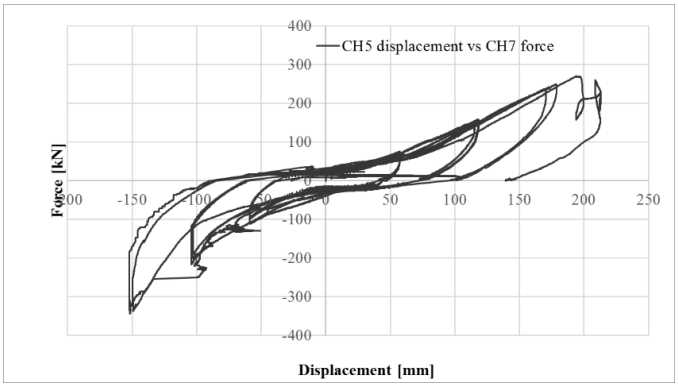



Fig. 19 CT1 – Transducer CH5 measurement.

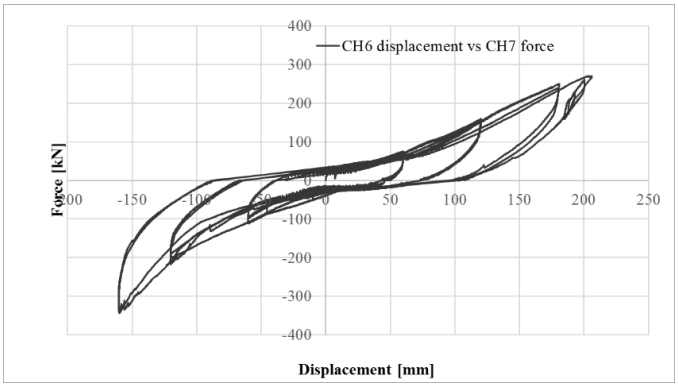



Fig. 20 CT1 – Transducer CH6 measurement.

The strain gauge findings corroborate the previously described connection failure. For instance, the results of 11SG (Fig. 21), positioned on the beam perpendicular to the dowel direction, exhibit relatively small strains, with a maximum value of 350μm/m. Visual inspection during the test verified that this area did not experience significant damage under loading. One potential drawback of strain gauges attached to concrete elements is that cracks might form outside the gauge area, leading to unrecorded relevant data or damaging the gauge if a substantial crack develops directly beneath it. A slight increase in strains is noticeable during the final cycles, but it is considerably smaller than the results of 13SG (Fig. 22), which are an order of magnitude higher (350μm/m versus 6500 μm/m). Strain gauge 13SG, located near the dowel on top of the column fork, registered the most significant damage through the final loading cycles and during the failure of the assembly.

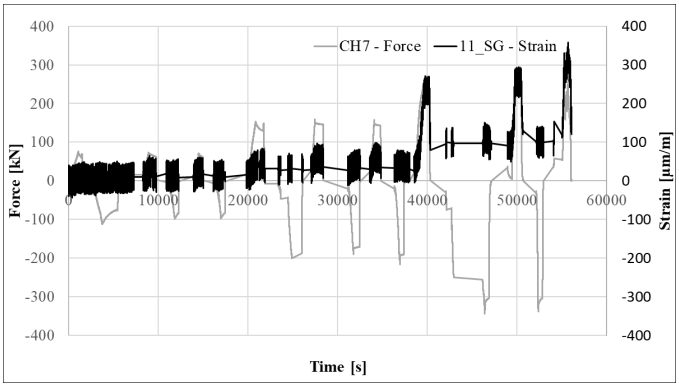



Fig. 21 CT1 – Strain gauge 11SG measurement.

Analysis of strain gauges 13SG and 14SG, situated on the column fork perpendicular to the dowel direction, reveals decreasing strains for gauges further from the connection. As illustrated in Fig. 13, concrete spalling occurred on the top side of the fork. However, 14SG still displays a significant strain value of 2500µm/m, confirming that the plastic hinge within the dowel shifts downward under higher loads. Outside this highly stressed area, recorded strains are an order of magnitude lower and nearly zero, with no significant change throughout the test, for this reason the results of these strain gauges are not shown. The maximum results recorded were 90 µm/m for 12SG, 60µm/m for 15SG and 40µm/m for 16SG.

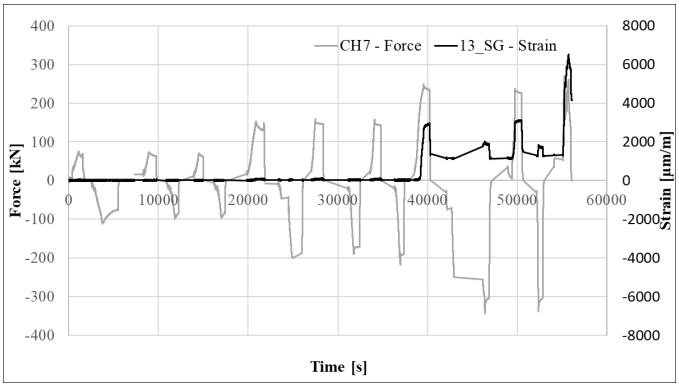



Fig. 22 CT1 – Strain gauge 13SG measurement.

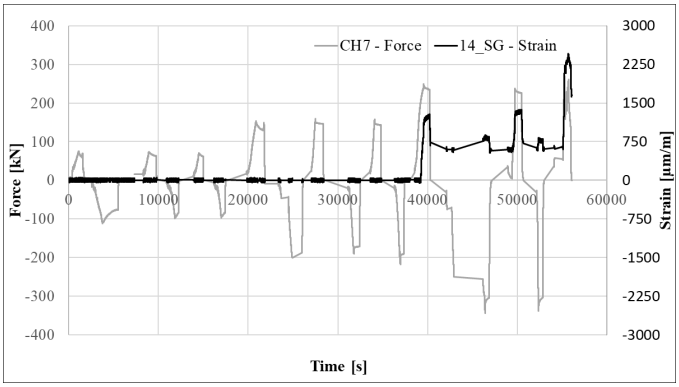



Fig. 23 CT1 – Strain gauge 14SG measurement.

Regarding strain results at the column bottom, recorded by 17SG (Fig. 24) and 18SG (Fig. 25) strain gauges, they exhibit lower values compared to 13SG. Maximum values at the column bottom range between 800µm/m and 1300µm/m, much lower than the 6500µm/m value recorded by 13SG. This suggests that the column base is not as stressed as the area surrounding the dowel, reinforcing the claim that the connection failed before any considerable damage was observed at the column base.

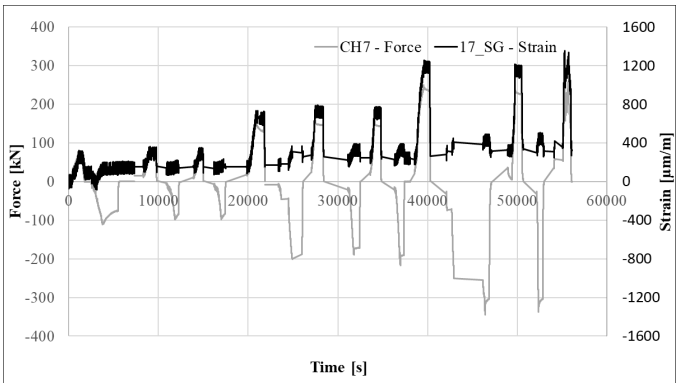



Fig. 24 CT1 – Strain gauge 17SG measurement.

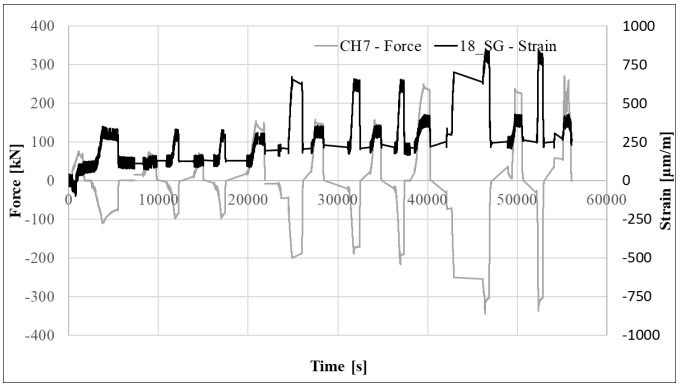



Fig. 25 CT1 – Strain gauge 18SG measurement.

## 4. Test results for the second cyclic test (CT2)

During the test specimen installation and connection casting process, a minor manufacturing inaccuracy regarding the beam sleeve position made it impossible to fully insert the dowels into the beam sleeve when connecting the beam and column elements. Consequently, the free length of the dowel between the two components was 3cm longer than planned—9cm instead of 6cm (Fig. 26). A greater dowel bending length can result in reduced connection strength, this was observed in the previous test after the dowel bond inside the column was damaged, resulting in an increased bending length.

The loading protocol employed was identical to that of CT1, as shown in Fig. 9. The test began with a tension load application, and the final load leading to failure was also a tension load which represents the most unfavourable loading case for this type of connection.

In this test, based on the results from the earlier test CT1, some strain gauge positions were altered. Since some strain gauges did not record significant data, it was decided to relocate them to areas where most of the damage was observed during prior tests. Damage was concentrated in the dowel area, causing concrete spalling at the column fork corners. Consequently, a strain gauge was placed on the front of the column fork, 15SG (Fig. 11). For the concrete beam, two strain gauges were positioned on the flange side, 11SG and 12SG (Fig. 11). In this test, the concrete coverage surrounding the sleeve within the beam was smaller, as previously mentioned, which could lead to crack formation also on the side of the beam.



Fig. 26 CT2 – Increased free length of the dowel.

Towards the end of the second series of load cycles (Fig. 9), with displacements up to 120mm, small cracks began to appear around the dowel in both the column fork and the beam end, in the dowel grouting (Fig. 27), at approximately 115kN in tension and 160kN in compression. In comparison to the previous test (CT1), these cracks developed earlier and, for the first time, began propagating within the beam element at higher loads.

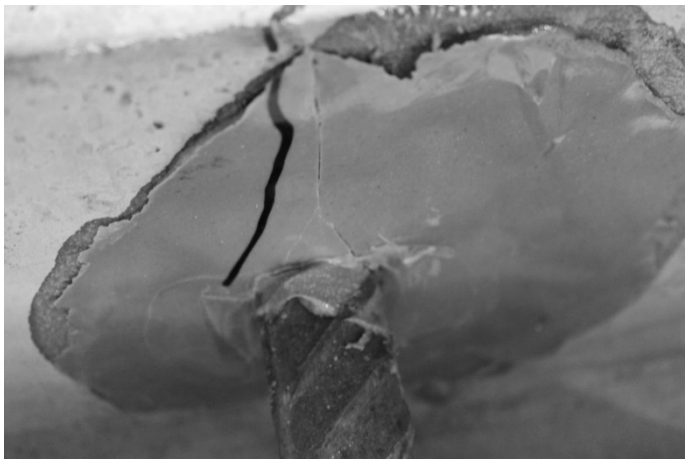


Fig. 27 CT2 – Crack in the grouting of the beam.

During the final cycles with displacements up to 180mm, cracks around the connection area expanded in both elements (Fig. 28 and Fig. 29) without noticeable damage elsewhere, indicating the connection was starting to fail. At

this stage, tension forces were around 190kN, while compression forces reached 300kN. The higher compression force resulted from the contact between the beam end and column fork, with the load transmitted through the concrete as well as the dowel.

The connection strength was significantly lower in tension, showing a 37% reduction due to load transmission through the dowel as shear forces and longitudinal forces caused by catenary action . Damage in the connection area was more severe than in the previous test, suggesting that lower concrete coverage substantially reduced connection capacity, particularly in the beam element.



Fig. 28 CT2 – Cracks expanding in the column fork.



Fig. 29 CT2 – Cracks expanding in the beam end, growing on the side of the flange.

Before failure, cracks in the beam expanded towards its end, appearing on both the web and flange of the elements (Fig. 30). The relative displacement between the column and beam was comparable to the previous test (CT1) until failure. The final tension load led to connection failure at approximately 245kN with a maximum imposed displacement of 210mm, causing sudden concrete spalling around the dowels and significant relative displacement between the elements. The failure mechanism was a combination of steel dowel yielding and concrete spalling (Fig. 31), with no significant damage observed at the column base. The reduced concrete cover for the dowels impacted the connection's capacity, resulting in a lower failure load compared to the previous cyclic test (CT1), which failed at a maximum load of 270kN.

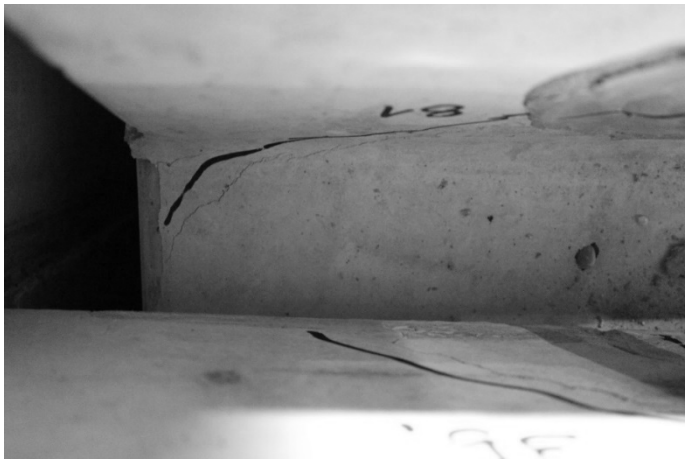


Fig. 30 CT2 – Cracks developing towards the end of the beam (flange and web).



Fig. 31 CT2 – Failure of the dowel connection.

Another crucial aspect is the dowel's increased free length, as previously mentioned and illustrated in Fig. 26. Damage was symmetrical on both sides of the elements.

The reduced concrete coverage effect is also evident in the beam end damage (Fig. 32), with large cracks extending to the back of the beam. This is a significant difference from previous tests where the beam remained unaffected at failure.



Fig. 32 CT2 – Extensive damage at the end of the beam.

Due to the lower failure load, the maximum crack width at the column base in the cross-section change area was smaller compared to CT1 results, with a value of 0.50mm versus 0.60mm. The final step exhibited a considerable relative displacement between the column and beam, with an approximate horizontal displacement of 6cm at failure. This may result from the increased dowel distance between the elements or the development of a plastic hinge within the beam sleeve. Examining the dowels after failure revealed greater deformation compared to previous tests, primarily due to the presence of two plastic hinges.

The results of the displacement transducers offer further insights into the failure mechanism and the behaviour of the entire testing assembly. In the case of relative displacement between the column and the beam, data from transducers CH1 (Fig. 33) and CH2 (Fig. 34) indicate smaller displacements in compression due to concrete element contact, which is more apparent for CH1. CH2 shows a lower relative displacement in compression because of the dowel connection at the top of the fork.

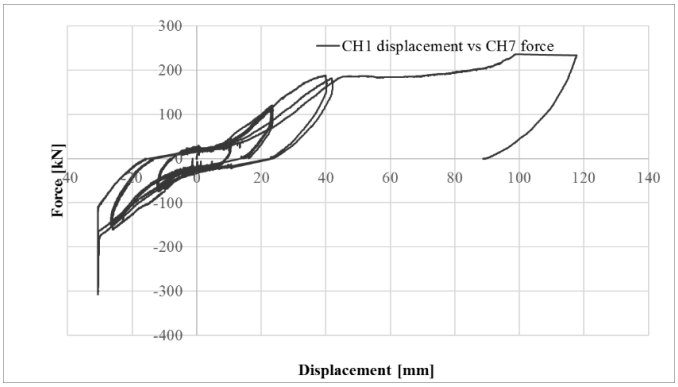



Fig. 33 CT2 – Transducer CH1 measurement.

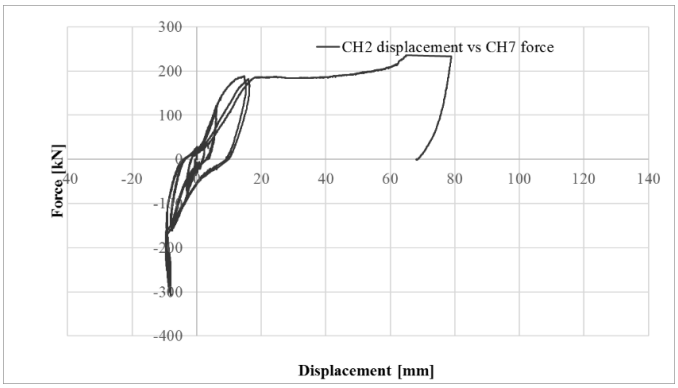



Fig. 34 CT2 – Transducer CH2 measurement.

In tension, recorded values are higher since the entire force is transmitted through the dowels. Before failure, both CH1 (Fig. 33) and CH2 (Fig. 34) display a large displacement corresponding to a small force increase, leading up to the concrete spalling. After this point, the force decreases with a sudden rise in displacement, indicating no remaining connection capacity, at this point the test was stopped for safety reasons.

Displacement transducers CH3 (Fig. 35) and CH4 (Fig. 36) recorded the unwanted rigid body rotation of the column due to the base fixing imperfection. These values will be used to calculate the rotation and extract it from the top column recordings during post-processing.

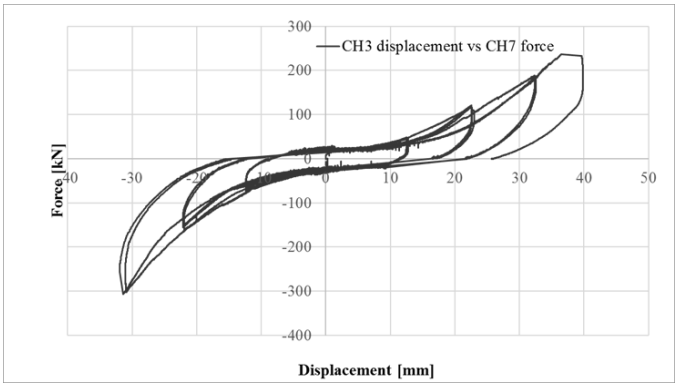



Fig. 35 CT2 – Transducer CH3 measurement

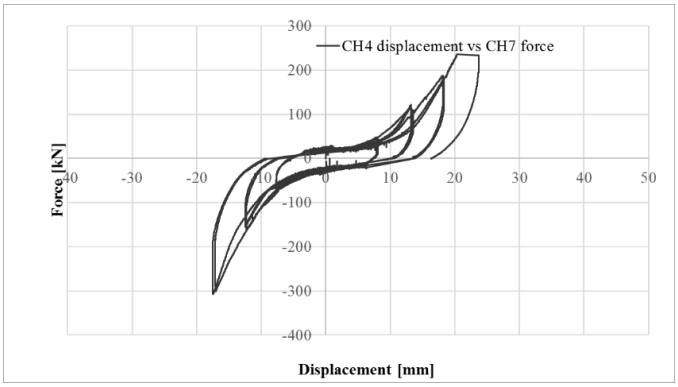



Fig. 36 CT2 – Transducer CH4 measurement

Data from CH5 (Fig. 37) and CH6 (Fig. 38) reveal the top displacement of the assembly. For CH5, a snapback occured after the connection failure, indicating that the connection was failing between 190mm and 220mm displacement under constant applied load. After the sudden failure, a short consolidation occured as forces redistributed. However, the connection could not withstand additional load, which lead to the halting of the test. CH6, which measured the top displacement of the column, shows an increase in displacement after reaching a 245kN failure load but at a lower force, potentially due to dowel consolidation after the sudden concreate spalling around it. Both CH5 and CH6 data demonstrate larger compressive forces due to concrete-to-concrete contact, with a maximum force of 300kN during the final loading cycle. However, friction force values affect these results, making it difficult to accurately estimate the actual failure load of the connection.

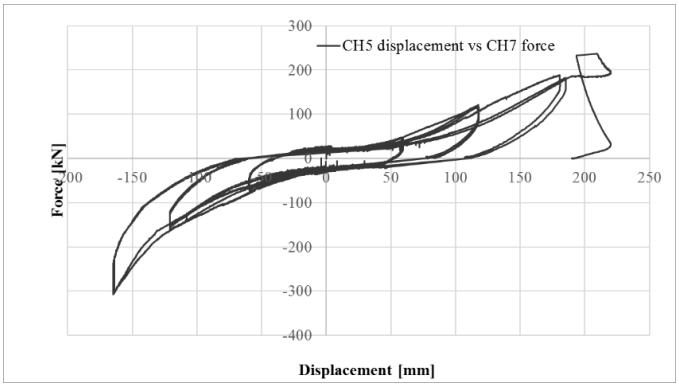
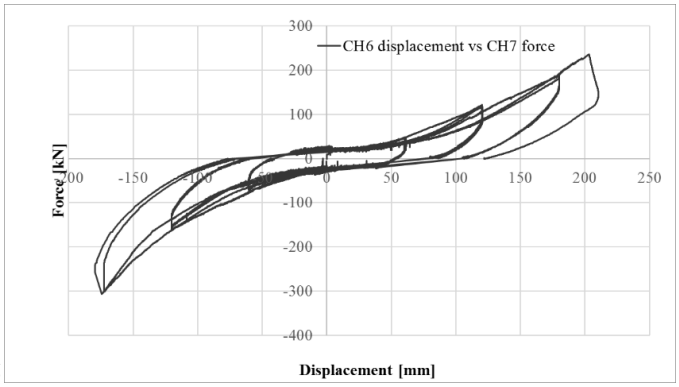



Fig. 37 CT2 – Transducer CH5 measurement




5

Fig. 38 CT2 – Transducer CH6 measurement

During the test, strain gauges near the dowel connection recorded the highest strain values. Data from 11SG (Fig. 39) and 12SG (Fig. 40) revealed large strains on the beam flange on the side of the element, confirming visual observations. Strain gauge 11SG (Fig. 39) recorded significantly higher values than 12SG (Fig. 40), this indicates that cracks propagated towards the back of the beam, where 11SG was located. In the previous cyclic test (CT1), no significant strain values were observed on the beam flange.Strain gauge 28SG (Fig. 41), situated on the top of the beam and perpendicular to the dowel direction, recorded a maximum value of 650μm/m. Cracks expanded towards the top of the beam as well, approaching the 28SG gauge. Strain gauges are highly sensitive to nearby crack formation, as confirmed by the lower values recorded by 12SG compared to 11SG data.

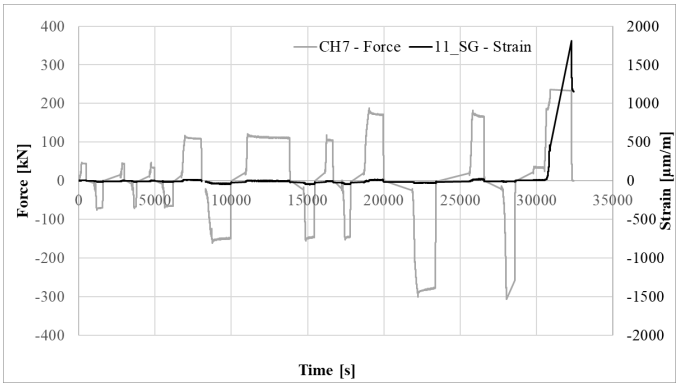



Fig. 39 CT2 – Strain gauge 11SG measurement

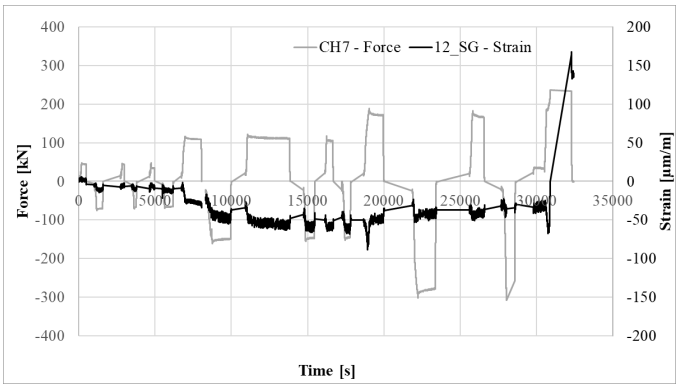



Fig. 40 CT2 – Strain gauge 12SG measurement

The highest strain value (4100µm/m) was observed top of the column fork by strain gauge 13SG (Fig. 42), where the first cracks developed around the dowel. The lateral side of the fork showed no significant strains, as evidenced by data recorded by the gauges 14SG and 16SG, with a maximum value of approximately 80µm/m for both, for this reason the graphs are not presented as they recorded mainly noise. Smaller concrete coverage of the dowel towards the interior of the fork led to the largest concentration of the damage in that area due to higher stress concentration. Strain gauge 15SG (Fig. 43), located on the front of the column fork and parallel to the dowel direction, recorded higher values (400µm/m) due to its proximity to the concrete spalling area in the interior corner of the fork (Fig. 31).

Data spikes at failure indicate a sudden connection failure, particularly for 11SG and 13SG. Strains for 28SG and 15SG developed incrementally during each cycle, as seen in the intermediate parts of the corresponding graphs.

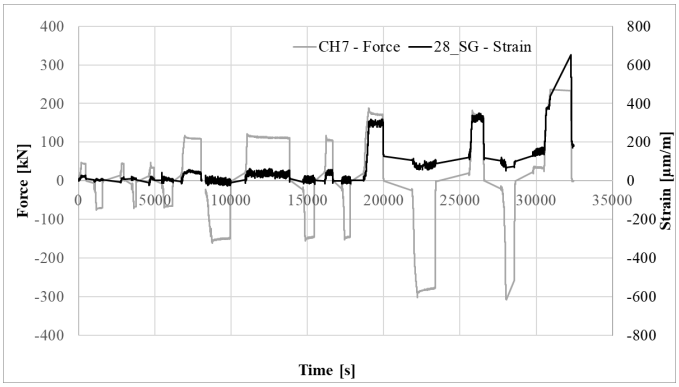



Fig. 41 CT2 – Strain gauge 28SG measurement

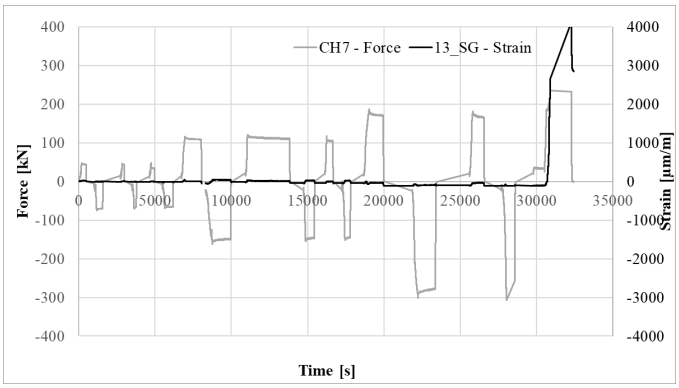



Fig. 42 CT2 – Strain gauge 13SG measurement

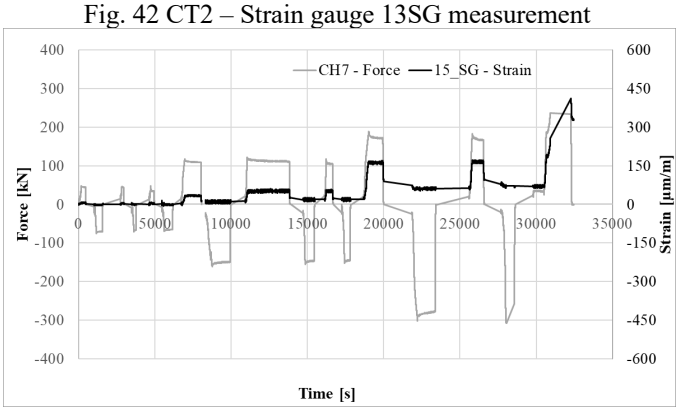



Fig. 43 CT2 – Strain gauge 15SG measurement

Higher strain values (1900-2200µm/m) were observed at the base of the column by the strain gauges 17SG (Fig. 44) and 18SG (Fig. 45). These values

increased incrementally during cyclic loading. Strain data at the base of the column is clearer due to uniform load distribution, unlike the results recorded near the connection with high concentrations of effects in small areas. Although, by comparing the maximum value from 17SG, it is 50% smaller than the maximum value recorded by 13SG, indicating connection failure before significant column damage. The results show similar behaviour to experiment CT1. In terms of absolute values, strain gauge results from the CT2 test displayed higher values at the base of the column compared to the CT1 test, even with a 10% smaller maximum load. As strain gauges are sensitive to nearby crack formation, it is possible that in CT2, cracks formed closer to the gauges or even as micro-cracks directly beneath them.

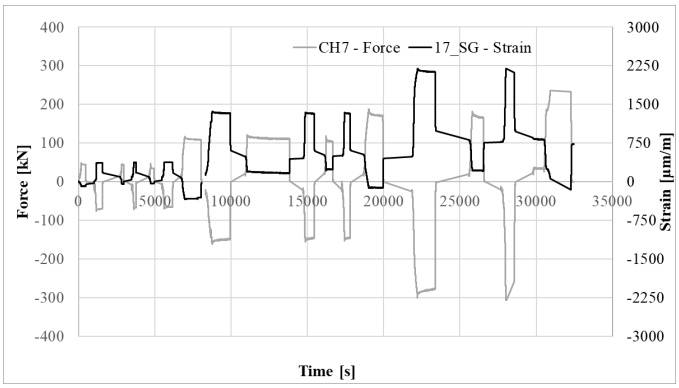



Fig. 44 CT2 – Strain gauge 17SG measurement

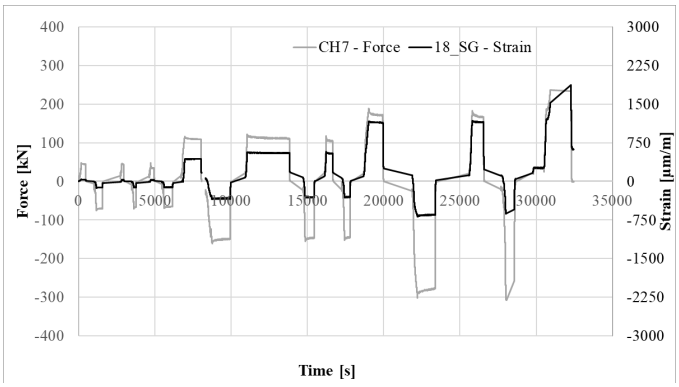



Fig. 45 CT2 – Strain gauge 18SG measurement

## 5. Conclusions

This study has investigated the behaviour and failure mechanism of the beam to column dowel connection under lateral cyclic loads. This was done through two cyclic tests on two different concrete coverage scenarios around the dowel. The key findings from the experiments are:

1. The assembly failure for both tests (CT1 and CT2) coincided with dowel connection failure in all experiments.
2. The CT1 assembly failure was associated with dowel yielding and concrete spalling in the column fork, occurring in tension at a load of 270 kN.
3. The CT2 assembly failure was associated with dowel yielding and concrete spalling of both column fork and beam flanges. The failure load for the second cyclic test, CT2, was 245 kN, which is 10% lower than that of CT1, due to reduced concrete coverages surrounding the dowel connector caused by alterations in the geometries of the connection area for the concrete elements.
4. No significant damage occurred in concrete elements outside the connection area, and the concrete column had minimal crack openings (<1mm) at the base.
5. The dowel connection failed to transmit sufficient lateral loads for the required dissipative failure mechanism in precast industrial halls, considered as inverted pendulum structures.
6. Ideally, in design considerations, the column base should develop a plastic hinge and dissipate the energy induced by the cyclic loading (or dynamic loading in an actual earthquake scenario) while the connection and the concrete area around the dowel remain elastic, transmitting horizontal forces to the column. However, the results demonstrate that the connection failed before the dissipative mechanism began developing in the column, as strains around the connection were more than four times larger.
7. Dowel connection capacity was influenced by concrete coverage in relation to column fork sides, with lower thickness resulting in smaller concrete coverages and lower failure loads.
8. Although large-scale tests are challenging and costly with limited data collection, the results can calibrate finite element models for additional information on element behaviour leading to assembly failure.

**Acknowledgements.**

The financial support by CONSOLIS is greatly acknowledged.

The research activities were supported by the project POCU/380/6/13/123927 – ANTREDOC, "Entrepreneurial competencies and excellence research in doctoral and postdoctoral studies programs", project co-funded from the European Social Fund through the Human Capital Operational Program 2014-2020.

## REFERENCES

Artioli, E., R. Battaglia, and A. Tralli. 2013. “Effects of May 2012 Emilia earthquake on industrial buildings of early ’900 on the Po river line.” Engineering Structures 56: 1220-1233.

Biondini, F., A. Titi, and G. Toniolo. 2012. “Pseudodynamic Tests and Numerical Simulations on a Full-Scale Prototype of a Multi-Storey Precast Structure.” 15WCEE. Lisboa.

Bournas, Dionysios A., Paolo Negro, and Francisco J. Molina. 2013. “Pseudodynamic tests on a full-scale 3-storey precast concrete building: Behavior of the mechanical connections and floor diaphragms.” Engineering Structures 57: 609-627.

Buratti, Nicola, Fabio Minghini, Elena Ongaretto, Marco Savoia, and Nerio Tullini. 2017. “Empirical seismic fragility for the precast RC industrial buildings damaged by the 2012 Emilia (Italy) earthquakes.” Earthquake Engng Struct. Dyn. 46 (14): 2317-2335.

Capozzi, V., G. Magliulo, and G. Manfredi. 2012. “Nonlinear Mechanical Model of Seismic Behaviour of Beam-Column Pin Connections.” 15WCEE. Lisboa.

Carydis, P., I. Psycharis, and H. Mouzakis. 2007. PRECAST EC8: seismic behaviour of precast concrete structures with respect to Eurocode 8. Final Report of the contribution of LEE/NTUA. FP5 Project No G6RD-CT-2002-00857.

CEN (Comité Européen de Normalisation). 2004. Eurocode 8: Design of structures for earthquake resistance – Part 1: General rules, seismic actions and rules for buildings (EN 1998-1). Brussels: CEN.

Cruz, Ana Maria, and Laura J. Steinberg. 2005. “Industry Preparedness for Earthquakes and Earthquake-Triggered Hazmat Accidents in the 1999 Kocaeli Earthquake.” Earthquake Spectra 21 (2): 285-303.

Demartino, Cristoforo, Ivo Vanzi, Giorgio Monti, and Concetta Sulpizio. 2018. “Precast industrial buildings in Southern Europe: loss of support at frictional beam-to-column connections under seismic actions.” Bull Earthquake Eng 16: 259–294.

Deyanova, Manya, Stefano Pampanin, and Roberto Nascimbene. 2014. “Assessment Of Single-Storey Precast Concrete Industrial Buildings With Hinged Beam-Column Connections With And Without Dowels.” Second European conference on earthquake engineering and seismology. Istanbul.

Ercolino, M., G. Magliulo, and G. Manfredi. 2016. “Failure of a precast RC building due to Emilia-Romagna earthquakes.” Failure of a precast RC building due to Emilia-Romagna earthquakes 118: 262-273.

European Comision. 2012. Design Guidelines for Connections of Precast Structures under Seismic Actions. Luxembourg: Joint Research Centre of the European Commission.

European Commission. 1999. COST Action C1 - Control of the semi-rigid behaviour of civil engineering structural connections. Luxembourg : Office for Official Publications of the European Communities.

Fischinger, Matej, Blaž Zoubek, and Tatjana Isakovic. 2014. “Chapter 4: Seismic Response of Precast Industrial Buildings.” Perspectives on European Earthquake Engineering and Seismology (Springer Cham Heidelberg New York Dordrecht London) 1 (34): 131-194.

Grimaz, Stefano, and Alberto Maiolo. 2010. “The Impact of the 6th April 2009 L’aquila Earthquake (italy) on the Industrial Facilities and Life Lines. Considerations in Terms of Natech Risk.” Chemical Engineering Transactions 19: 279-284.

Karadogan, F, E Yuksel, and I E Bal. 2012. “The Seismic Behavior of An Asymmetric Exterior Precast Beam-Column Connection.” 15 WCEE. Lisboa.

Keronen, A., and J. Hietala. 1998. “TESTS AND ANALYSIS OF THE CONNECTIONS IN PRECAST CONCRETE PORTAL FRAME.” COST C1 : Control of the semi-rigid behaviour of civil engineering structural connections. Liège.

Kremmyda, Georgia D., Yasin M. Fahjan, and Spyros G. Tsoukantas. 2014. “Nonlinear FE analysis of precast RC pinned beam-to-column connections under monotonic and cyclic shear loading.” Bulletin of Earthquake Engineering 12: 1615-1638.

Liberatore, Laura, Luigi Sorrentino, Domenico Liberatore, and Luis D. Decanini. 2013. “Failure of industrial structures induced by the Emilia (Italy) 2012 earthquakes.” Engineering Failure Analysis 34: 629-647.

Magliulo, Gennaro, Davide Bellotti, Maddalena Cimmino, and Roberto Nascimbene. 2018. “Modeling and Seismic Response Analysis of RC Precast Italian Code-Conforming Buildings.” JOURNAL OF EARTHQUAKE ENGINEERING 22: 140-167.

Magliulo, Gennaro, Giovanni Fabbrocino, and Gaetano Manfredi. 2008. “Seismic assessment of existing precast industrial buildings using static and dynamic nonlinear analyses.” Engineering Structures 30: 2580-2588.

Magliulo, Gennaro, Marianna Ercolino, Crescenzo Petrone, Orsola Coppola, and Gaetano Manfredia. 2014. “The Emilia Earthquake: Seismic Performance of Precast Reinforced Concrete Buildings.” Earthquake Spectra 30 (2): 891-912.

Magliulo, Gennaro, Marianna Ercolino, Maddalena Cimmino, Vittorio Capozzi, and Gaetano Manfredi. 2014. “FEM analysis of the strength of RC beam-to-column dowel connections under monotonic actions.” Construction and Building Materials 69: 271-284.

Magliulo, Gennaro, Vittorio Capozzia, Giovanni Fabbrocino, and Gaetano Manfredi. 2011. “Neoprene–concrete friction relationships for seismic assessment of existing precast buildings.” Engineering Structures 33: 532-538.

MSZ EN. 2014. “MSZ EN 12390-13:2014, Testing hardened concrete. Determination of secant modulus of elasticity in compression.”

MSZ EN. 2015. “MSZ EN 12390-3:2015, Testing hardened concrete. Compressive strength of test specimens.”

MSZ EN. 2009. “MSZ EN 12390-5:2009, Testing hardened concrete. Flexural strength of test specimens.”

Nigel Priestley, M. J. 1996. “The PRESSS Program - Current Status and Proposed Plans for Phase Ill.” PCI Journal 44 (2): 22-40.

Pollini, Andrea Vittorio, Nicola Buratti, and Claudio Mazzotti. 2021. “Behavior factor of concrete portal frames with dissipative devices based on carbon wrapped steel tubes.” Bulletin of Earthquake Engineering 19: 553–578.

Psycharis, N. Ioannis, and P. Harris Mouzakis. 2012. “Shear resistance of pinned connections of precast members to monotonic and cyclic loading.” Engineering Structures 41: 413-427.

Senel, Sevket Murat, and Ali Haydar Kayhan. 2010. “Fragility based damage assesment in existing precast industrial buildings: A case study for Turkey.” Structural Engineering and Mechanics 34 (1): 39-60.

Sika Services AG. 2019. Product Data Sheet for Sika AnchorFix-3030. Zürich. https://industry.sika.com/en/home/renewable-energies/wind-energy/concrete-tower/anchoring/sika-anchorfix-3030.html.

Sørensen, Jesper H., Linh C. Hoang, John F. Olesen, and Gregor Fischer. 2017. “Testing and modeling dowel and catenary action in rebars crossing shear joints in RC.” Engineering Structures 145: 234-245.

Task Group 6.12: fib Design Handbook. 2014. Planing and design handbook on precast building structures. Lausanne: International Federation for Structural Concrete.

Titi, Andrea, Fabio Biondini, and Giandomenico Toniolo. 2018. “Seismic assessment of existing precast structures with dry-friction beam-to-column joints.” Bull Earthquake Eng 16: 2067–2086.

Toniolo, G. 2012. “European research on seismic behaviour of precast structures.” NZSEE. Lausanne.

Zoubek, Blaž, Matej Fischinger, and Tatjana Isakovic. 2015. “Estimation of the cyclic capacity of beam-to-column dowel connections in precast industrial buildings.” Bulletin of Earthquake Engineering 13 (7).

Zoubek, Blaz, Tatjana Isakovic, Yasin Fahjan, and Matej Fischinger. 2013. “Cyclic failure analysis of the beam-to-column dowel connections in precast industrial buildings.” Engineering Structures 52: 179–191.

# ANALIZA EXPERIMENTALA CICLICA A UNEI CONEXIUNI GRINDA-STALP

(Rezumat)

Acest studiu investighează comportamentul și mecanismul de cedare sub sarcini laterale a unei conexiuni cu dornuri de tip grindă-stâlp utilizată frecvent la hale industriale prefabricate din beton armat. Au fost efectuate două teste ciclice la scară reală pentru a evalua comportamentul ansamblului prefabricat. Rezultatele au demonstrat că cedarea ansamblului coincide cu cedarea conexiunii cu dornuri, aceasta fiind cauzată de cedarea la încovoiere și forfecare a dornurilor și de desprinderea betonului din furca stâlpului. Nu au fost observate deteriorări semnificative în elementele de beton în afara zonei de conexiune. Mecanismul de cedare disipativă a stâlpului nu a fost activat, ceea ce indică faptul că această conexiune cu dornuri nu a putut transmite suficiente sarcini laterale pentru a satisface această cerință. Capacitatea maximă a conexiunii cu dornuri a fost influențată de stratul de acoperire cu beton a dornurilor în raport cu partea laterală a furcii stâlpului. Această analiză servește drept bază pentru investigații suplimentare și potențiale îmbunătățiri în proiectarea și performanța conexiunilor la construcții prefabricate din beton armat.